Phosphate removal from water using bottom ash: adsorption performance, coexisting anions and modelling studies

Khalid S. Hashim, Hind Mufeed Ewadh, Adnan A. Muhsin, Salah L. Zubaidi, Patryk Kot, Magomed Muradov, Mohammed Aljefery and Rafid Al-Khaddar

ABSTRACT

Phosphate in freshwater possesses significant effects on both quality of water and human health. Hence, many treatment methods have been used to remove phosphate from water/wastewaters, such as biological and electrochemical methods. Recent researches demonstrated that adsorption approaches are convenient solutions for water/wastewater remediation from phosphate. Thus, the present study employs industrial by-products (bottom ash (BA)), as a cost-effective and eco-friendly alternative, to remediate water from phosphate in the presence of competitor ions (humic acid). This study was initiated by characterising the chemical and physical properties of the BA, sample, then Central Composite Design (CCD) was utilised to design the required batch experiments and to model the influence of solution temperature (ST), humic acid concentration (HAC), pH of the solution (PoS) and doses of adsorbent (DoA) on the performance of the BA. The Langmuir model was utilised to assess the adsorption process. The outcomes of this study evidenced that the BA removed 83.8% of 5.0 mg/l of phosphates at ST, HAC, PoS and DoA 35 °C, 20 mg/L, 5 and 55 g/L, respectively. The isotherm study indicated a good affinity between BA and phosphate. Additionally, the developed model, using the CCD, reliably simulated the removal of phosphates using BA ($R^2 = 0.99$).

Key words | adsorption, furnace bottom ash, industrial by-products, phosphate

HIGHLIGHTS

- Fresh bottom ash from power production plants was used as an adsorbent for phosphate.
- The new adsorbent removed 83.8% of phosphate in a short time.
- The performance of the new adsorbent was modelled using the CCD method.
- Isotherm models were used to understand the nature of the adsorption process.

Khalid S. Hashim (corresponding author)
Patryk Kot
Magomed Muradov
Mohammed Aljefery
Rafid Al-Khaddar
Built Environment and Sustainable Technologies (BEST) Research Institute,
Liverpool John Moores University,
Liverpool L3 3AF,
UK
E-mail: *k.s.hashim@ljmu.ac.uk*

Khalid S. Hashim
Faculty of Engineering,
University of Babylon,
Hilla, 5200,
Iraq

Hind Mufeed Ewadh
Environmental Research and Studies Center,
University of Babylon,
Hilla, 52001,
Iraq

Adnan A. Muhsin
Al-Furat Al-Awsat Technical University, Al-Mussaib Technical Institute,
Babylon, 51009,
Iraq

Salah L. Zubaidi
Department of Civil Engineering,
Wasit University,
Wasit, 51001,
Iraq

doi: 10.2166/wst.2020.561

GRAPHICAL ABSTRACT

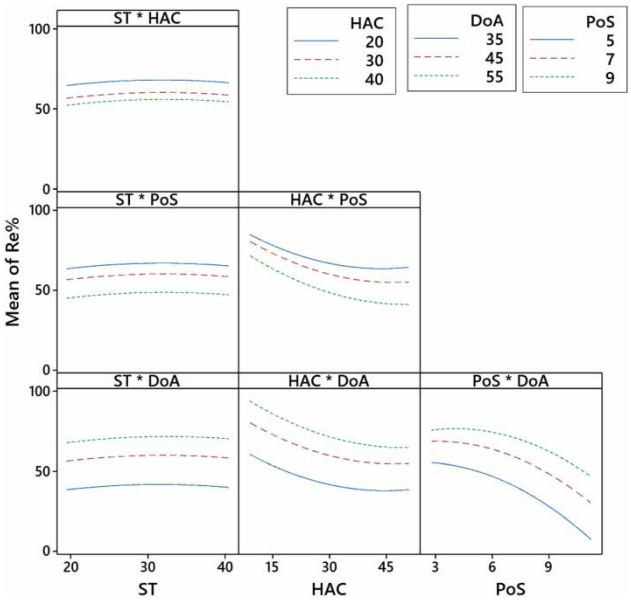

INTRODUCTION

The agricultural industry has witnessed substantial changes during the last half-century to meet the soaring demands for foods and fibers (Zalidis *et al.* 2002; Alwash 2017), which results in a substantial deterioration of freshwater sources (Withers *et al.* 2014; Zhao *et al.* 2015; Omran *et al.* 2019). For instance, agriculture contributes to 60% of nitrate and 25% of phosphate in the freshwater sources in the United Kingdom, and about 75% of sediments contaminating freshwater sources worldwide (Holden *et al.* 2015). In addition, it results in huge economic losses; for instance, the eutrophication of freshwaters in England and Wales due to the occurrence of phosphorus, which resulted in annual losses of $105,000,000 and $160,000,000, respectively. Generally, there are two main ways to transport phosphate from agricultural landscapes to the sources of freshwaters: surface runoffs and sub-surface flows (Sellner 2016). It was believed that the surface runoffs are the main way for transporting phosphate from farms to the receiving water bodies; however, recent studies have evidenced that sub-surface flow is the predominant means of phosphate transportation from farms to the sources of freshwaters (King *et al.* 2015). For example, King *et al.* (2015) conducted a study for 8 years to estimate the contribution of sub-surface flow to the total phosphate in central Ohio; the results of their study proved that sub-surface flow is responsible for 48% of the total phosphate in that area, and also proved that ≥90% of the measured concentrations were ≥0.02 mg/L. It must be mentioned that the agricultural activities are not the only origin of phosphate in the aquatic environment; considerable concentrations of phosphate could be found in the domestic and industrial effluents (Alwash 2017).

To mitigate phosphate discharging into the sources of freshwaters and to avoid further deterioration of freshwater sources and phosphate-related health problems, effective treatment approaches must be used to remove phosphate from effluents. To solve this dilemma, the specialists have suggested a number of complex or simple technologies, such as nanomaterial-based methods, biological reactors and wetlands, electrochemical reactors, artificial absorbents and natural absorbents (Dai & Pan 2014; Park *et al.* 2015; Alwash 2017; Kumar *et al.* 2019). Adsorption technology, which is based on the sorption of phosphate on low-cost artificial or natural and by-product adsorbents, has been recently recognized as a promising method for remediation of water not only from phosphate but also from a broad spectrum of contaminants. For instance, by-products of steel and iron factories, limestone, calcite, zeolites, exfoliated vermiculites, ferric hydroxide, nanoparticles of

different materials, and activated carbons (derived from artificial or natural origins) were employed in the literature to remediate waters from phosphate (Alwash 2017; Kumar et al. 2019). Generally, any material with rich content of aluminium, magnesium, calcium, or/and iron oxide is favourable in the phosphate adsorption process as the oxides have the capacity to provide cations for phosphate to react with. The latter reaction, between phosphate and cations, yields insoluble compounds, which could be easily separated from the solutions being treated (Sellner 2016). A promising phosphate sorption material is the by-products of the coal burning process (in furnaces) as the latter is usually rich with one or more of the mentioned oxides (Kirk et al. 2003). By-products of coal burning are divided into two types: the first is very small in size and has a light weight, thus it escapes the combustion chamber through the chimney, and is known as fly ash. The second type, which is known as bottom ash (BA), mainly consists of inorganic and non-combustible particles that remain in the bottom of the combustion chamber due to their relatively heavy weight and large size (Kirk et al. 2003). Although BA is rich in iron and aluminium oxides, the majority of BA is wasted in landfills (Hjelmar et al. 2010) that requires expensive land and transportation investments. However, due to the attractive chemical composition and free availability of BA, some trials have been made to recycle it in some applications, such as the concrete industry (Zhang & Poon 2015; Shubbar et al. 2018). However, to the best of the authors' knowledge, fresh BA from power plants has not been used in water treatment yet. Few trials were made to use nano-powder of BA in water treatment (Alwash 2017), which have limited applications due to the high production cost (production of nanopowder) and the safety concerns (Tyagi et al. 2018).

In the present study, the BA has been utilised as an economically efficient adsorbent for phosphate. The selection of the BA here is due to two main reasons: firstly, because the BA is rich in iron aluminium oxides (as stated in the results section of this study), that gives it a good potential capacity for phosphate sorption. Secondly, the BA itself is classified as an industrial by-product that is environmentally harmful and it usually requires expensive management plans (Jamaludin et al. 2019). Thus, utilising this by-product in water treatment is environmentally and economically beneficial. To have a preliminary decision about the applicability of AB for remediation of water from phosphate, several batch experiments were commenced taking into account the influences of solution temperature (ST), humic acid concentration (HAC), pH of the solution (PoS) and dose of adsorbent (DoA). It is noteworthy to mention that humic acid has been used here to mimic the effects of competitor ions in the field works. Humic acid was used as a competitor ion model here due to its wide occurrence in freshwaters and wastewaters (Han et al. 2017).

METHODOLOGY

Characterization of the BA sample

The sample of BA was obtained from a local power station in England, UK. The key chemical and physical properties of the collected BA sample were examined before applying it for phosphate removal from water; the studied properties were the grain size distribution, coefficient of uniformity (CU), coefficient of gradation (CG), surface area, specific gravity, and chemical composition.

Sieve analysis was used to measure the grain size distribution; a measured weight of BA, 0.25 kg, was sieved using a set of sieves (No.6, No.10, No.16, and No.30 top-to-bottom) using a bench-scale shaker (model: Impact SV-003). The retained weight of BA on each sieve was measured to estimate the grain size distribution. The measured weights were used to calculate the CU (Equation (1)) and CG (Equation (2)); well-graded samples have CU> 4.0 and CG in the range 1–3 (Viswanadham 2016).

$$\mathrm{CU} = \frac{\mathrm{d}_{60}}{d_{10}} \tag{1}$$

$$\mathrm{CG} = \frac{d_{30}^2}{d_{10} \times d_{60}} \tag{2}$$

where d_{60} is the grain size that 60 percent of other grains are finer than it, d_{10} is the grain size that 10 percent of other grains are finer than it, and similarly d_{30} is the grain size that 30 percent of other grains are finer than.

The specific surface area of BA particles has been measured as it determines the number of active sites, which directly affects the adsorption efficiency. In the present study, a surface area analyser (Quantachrome Nova-2000) was employed to determine the specific surface area of the BA particles. In this process, the BA sample was out-gassed with pure N_2 for 12.0 hours at a temperature of 300 °C (Boonamnuayvitaya et al. 2005). Then the recorded data was applied to Equations (3) and (4) to calculate the

specific surface area of the BA sample (Gregg & Sing 1982).

$$\text{Surface area} = \frac{X_m \times L_{av} \times A_m}{M_v} \quad (3)$$

$$\text{Specific surface area} = \frac{\text{Surface area}}{\text{weight of sample}} \quad (4)$$

where X_m, L_{av}, $A_{m,}$ and M_v are the monolayer capacity, Avogadro's number, the cross-sectional area of the adsorbent, and the molar volume, respectively. The chemical composition of BA was analysed using an X-ray fluorescence analyser (Shimadzu EDX-720). This test was run to calculate the concentrations of oxides and trace elements in the BA sample.

Batch experiments

A suitable amount of mono-potassium phosphate, 7.17 mg, was dissolved in deionized water to produce 5 mg/L phosphate solution, which was polluted with different concentrations of humic acid (10 to 50 mg/L), as competitor ions, using a suitable amount of humic acid sodium salt. It is noteworthy to mention that humic acid has been chosen as a model for competitor ions as it broadly occurs in freshwaters (Han *et al.* 2017). The simulated phosphate-humic acid solution was treated BA.

For each experiment, the BA and phosphate-humic acid solution were mixed at different ratios (40 to 60 g/L), then the mixture was shaken, using a bench-top shaking incubator (Model: Labnet-222DS) at a speed of 100 rpm for 24 hours (Sellner 2016). The residual phosphate concentration in solution was measured by filtering a few millimetres in a 0.45μm filter and analysed using standard phosphate cuvette tests (LCK-349 and 350) and a spectrophotometer (DR-2800). It is noteworthy to mention that to measure the concentration of humic acid using the spectrophotometer, a calibration curve was first developed for the concentration range 0 to 50 mg/L. The equilibrium adsorption capacity, *qe* (mg/g), was measured as follows (Sellner 2016):

$$q_e\left(\frac{mg}{g}\right) = \frac{V(C_i - C_e)}{m} \quad (5)$$

$$\text{Removal efficiency (Re\%)} = \frac{(C_i - C_e)}{C_i} \times 100\% \quad (6)$$

where C_i and C_e are the initial and equilibrium phosphate concentrations (mg/L), respectively, m is the amount of BA (grams), V is the volume of phosphate-humic acid solution (litters).

Adsorption isotherm

It is very essential, in the adsorption studies, to assess the relationship between the adsorbed and aqueous concentrations at the equilibrium status. Many isotherm models could be used to assess this relationship, such as the Langmuir and Freundlich models (Alwash 2017). In the present study, the Langmuir model, Equation (7), has been applied to assess the relationship between the adsorbed and aqueous concentrations of phosphate not only because this model is the most widely used one, but also it delivers the required parameters to determine the separation factor (R_L), which is represented by Equation (8) (Al-Othman *et al.* 2012). The latter gives a direct assessment for the affinity between the absorbate and absorbent; the adsorption process is unfavourable, linear, favourable, or irreversible when $R_L > 1$, $R_L = 1$, $1 > R_L > 0$, and $R_L = 0$, respectively (Dada *et al.* 2012).

$$\frac{C_e}{q_e} = \frac{1}{Q_o \times b} + \frac{C_e}{Q_o} \quad (7)$$

$$R_L = \frac{1}{1 + b \times C_i} \quad (8)$$

where Q_o and b represents the theoretical mono-layer adsorption (mg/g) and the energy of adsorption (L/mg), respectively. The values of Q_o and b can be obtained from the plot of the Langmuir model (C_e/q_e against C_e); Q_o and b are obtained from the slopes and intercepts of the mentioned plot, respectively. In the present study, the Langmuir model was performed by mixing 100 ml of phosphate solution with different amounts of BA (1.5 to 6.5 g/L), in airtight containers, and shaking for 24 hours at speed of 100 rpm to reach the equilibrium status. The results were plotted to get the required information to calculate R_L.

Optimisation and modelling of phosphate adsorption

The adsorption process was optimised using Central Composite Design (CCD), which is a member of the Response Surface Methodology. The CCD was performed using the Minitab package (version 19), and the optimisation process covered the influences of solution temperature (ST), humic acid concentration (HAC), pH of the solution (PoS), and doses of adsorbent (DoA) on the adsorption process. The

studied ranges of the PoS, ST, HAC, and DoA are tabulated in Table 1. The incubator was used to adjust the ST to the desired value (20–40 °C), while the PoS was adjusted to the range of 3–11 using NaOH or HCl solution. Additionally, a regression analysis was performed to assess the significance of each of the studied parameters in the adsorption of phosphate on the BA particles.

Performing CCD yielded 31 experimental runs, see Table 2, which are essential to attain the optimum performance of the BA filter in terms of phosphate removal under the mentioned conditions, and also this number of experiments are necessary to develop a simulation model for phosphate removal by BA.

Table 1 | Ranges of the studied parameters

		Ranges				
Parameter	**Unit**	**−2**	**−1**	**0**	**+1**	**+2**
ST	°C	20	25	30	35	40
HAC	mg/l	10	20	30	40	50
PoS	Unitless	3	5	7	9	11
DoA	g/L	25	35	45	55	65

Table 2 | Experimental runs according to CCD

Runs	**ST**	**HAC**	**PoS**	**DoA**	**Runs**	**ST**	**HAC**	**PoS**	**DoA**
1	30	30	7	45	17	35	20	9	55
2	30	30	7	45	18	30	30	7	65
3	25	40	9	55	19	25	40	5	35
4	35	40	5	55	20	25	40	9	35
5	30	30	7	45	21	35	20	9	35
6	35	20	5	35	22	35	20	5	55
7	35	40	5	35	23	30	30	3	45
8	30	30	7	25	24	30	50	7	45
9	20	30	7	45	25	30	30	7	45
10	25	20	9	35	26	30	30	7	45
11	35	40	9	55	27	35	40	9	35
12	30	30	7	45	28	30	30	7	45
13	40	30	7	45	29	30	30	11	45
14	25	20	5	55	30	25	40	5	55
15	30	10	7	45	31	25	20	9	55
16	25	20	5	35					

RESULTS AND DISCUSSION

Characterization of the BA sample

As was mentioned above, the physical and chemical properties of the BA sample determine its suitability for the adsorption process. Therefore, the chemical composition and physical properties (grain size distribution, CU, CG, surface area, and specific gravity) have been examined.

The chemical composition analyses of BA has revealed considerable concentrations of aluminium, iron, calcium, and magnesium oxides, which are favourable for phosphate removal. According to the listed results in Table 3, about 18.287% of the chemical composition of BA consists of the mentioned oxides, which confirms that this by-product is suitable for phosphate adsorption.

Table 4 shows the physical properties of BA, which confirm that the physical properties of the BA sample are suitable for the adsorption process; the BA sample is well-graded as its CU was more than 4.0 and its CG was in the range of 1–3 (Viswanadham 2016). Additionally, the specific gravity of BA is bigger than that of water, which means it will not float during the adsorption process.

Batch experiments

Phosphate removal experiments have been carried out according to the presented experimental design in Table 2. The obtained results are presented in Table 5 and Figure 1. According to the obtained results, maintaining the PoS in

Table 3 | Chemical composition of BA

Oxide	**Percentage**	**Oxide**	**Percentage**
Al_2O_3	9.953	CHO	60.381
Fe_2O_3	6.321	BaO	0.193
CaO	1.301	SO_3	0.191
MgO	0.712	SrO	0.052
SiO_2	19.301	CO_2O_3	0.0162
K_2O	0.753	ZrO_2	0.016
TiO_2	0.272	MnO	0.038

Other trace elements represent less than 0.005% of the chemical composition of BA.

Table 4 | Physical properties of BA

Parameter	**CU**	**CG**	**Specific gravity**	**Surface area (m^2/g)**
Value	5.450	1.369	1.285	5

Table 5 | Removal of phosphate using BA

Runs	ST	HAC	PoS	DoA	Re. (%)	Runs	ST	HAC	PoS	DoA	Re. (%)
1	30	30	7	45	60.3	17	35	20	9	55	72.8
2	30	30	7	45	60.0	18	30	30	7	65	77.4
3	25	40	9	55	54.2	19	25	40	5	35	47.6
4	35	40	5	55	72.7	20	25	40	9	35	22.4
5	30	30	7	45	59.9	21	35	20	9	35	36.1
6	35	20	5	35	57.3	22	35	20	5	55	83.8
7	35	40	5	35	48.4	23	30	30	3	45	68.4
8	30	30	7	25	17.1	24	30	50	7	45	55.2
9	20	30	7	45	57.4	25	30	30	7	45	60.0
10	25	20	9	35	35.3	26	30	30	7	45	59.9
11	35	40	9	55	55.8	27	35	40	9	35	24.1
12	30	30	7	45	59.8	28	30	30	7	45	60.1
13	40	30	7	45	57.8	29	30	30	11	45	32.7
14	25	20	5	55	82.1	30	25	40	5	55	71.2
15	30	10	7	45	78.7	31	25	20	9	55	71.4
16	25	20	5	35	56.4						

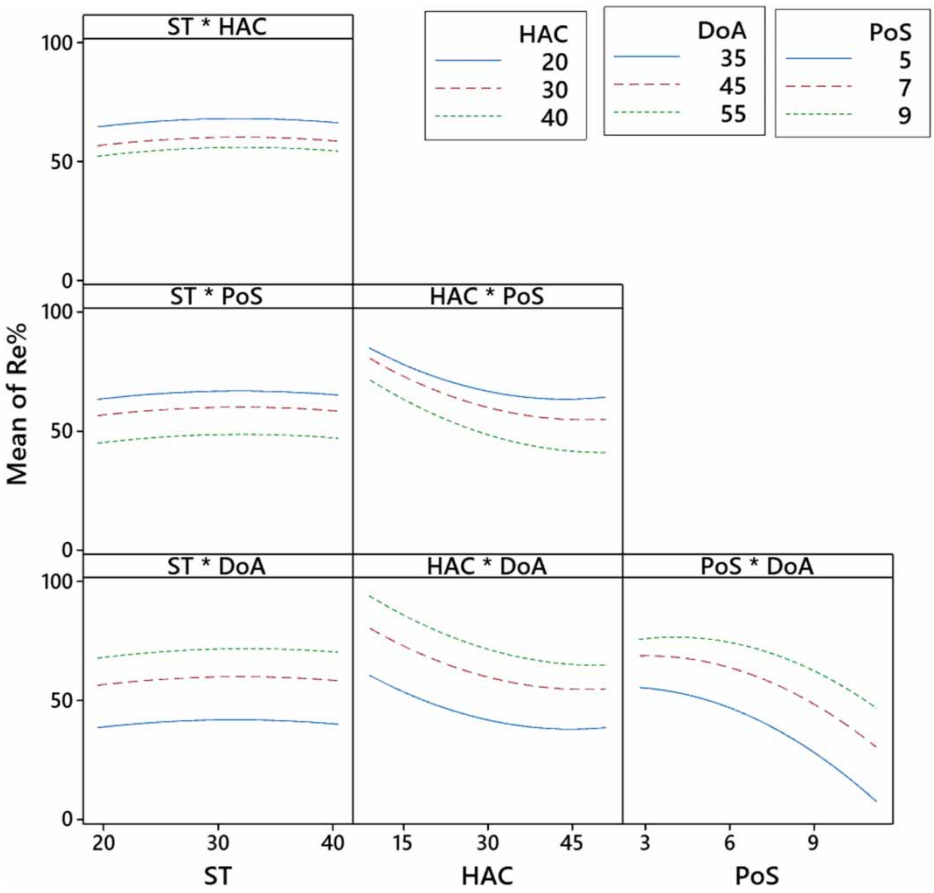

Figure 1 | Interaction between phosphate removal and ST, HAC, PoS and DoA.

the acidic range resulted in better removal of phosphate in comparison with neutral and alkaline ranges. For instance, the removal of phosphate decreased from 68.4% to 59.9% and 32.7% as the PoS increased from 3 to 7 and 11, respectively, when the ST, HAC, and DoA were kept constant at 30 °C, 30 mg/L, and 45 mg/L, respectively. The lower phosphate adsorption on the alkaline medium is probably because at the higher PoS, the absorbent particles carry more negative charges, which intensifies the repulsion between the absorbent particles and negatively charged phosphate ions (Alwash 2017). Other researchers attributed the lower phosphate adsorption on the alkaline medium to the increase in adsorption of OH- ions onto the absorbent, decreasing the availability of adsorption sites for phosphate (Sellner 2016). The literature (Sellner 2016; Alwash 2017) demonstrated similar effects of PoS on phosphate removal by adsorption method.

The results obtained from the experimental work evidenced that the occurrence of coexisting ions, humic acid, exerted negative impacts on the adsorption of phosphate by BA particles, especially at high concentrations. It can be obviously seen from the results of Table 5 and Figure 1 that increasing the HAC from 10 to 50 mg/L shrank the removal of phosphate by about 24%, when the ST, PoS, and DoA were kept constant at 30 °C, 7 and 45 mg/L, respectively. According to the literature, there are three possible reasons for this shrinking in phosphate removal with the increase of HAC: (i) the competitive adsorption of humic acid and phosphate onto the surfaces of BA particles; (ii) the accumulation of organic matter on the surface of the adsorbent weakens or changes the surface charge of adsorbent, which minimises the electrostatic attraction; and (iii) organic matter could delay or inhibit the chemical reactions between phosphate and aluminium and iron oxides (Borggaard *et al.* 2005; Sellner 2016; Amini *et al.* 2020). The literature showed similar effects of humic acid on phosphate adsorption onto different types of adsorbents, such as iron oxides (Weng *et al.* 2012).

Solution temperature (ST) has a substantial role in the adsorption process at liquid-solid interfaces as it determines the driving force of phosphate ions onto the surfaces of the adsorbents, and it also affects the energy barriers of reactions between the adsorbents and the adsorbates (Liu *et al.* 2011). Therefore, the effects of ST on phosphate uptake by the BA particles have been examined at several temperature levels, ranging from 20 to 40 °C. According to the results of Table 5 and Figure 1, the uptake capacity of BA for phosphate is positively influenced by the increase of ST to a certain limit; an increase in the uptake of phosphate in ST range of 20 to 35 °C, but a slight decrease was noticed in the uptake of phosphate when ST increased to 40 °C when the HAC, PoS, and DoA were kept constant at 30 mg/L, 7 and 45 mg/L, respectively. For example, the removal of phosphate increased from about 57% to 60% as the ST increased from 20 to 30 °C, respectively. However, increasing the ST from 30 to 40 °C decreased the removal of phosphate from 60% to about 58%, respectively. According to previous studies, there are several reasons behind the increase in the uptake of phosphate with the increase of ST; increasing the bulk temperature expands the pore size on the surface of the adsorbents, which increases the adsorption capacity (Alwash 2017). Another reason is that the increase of ST maximises the driving force of phosphate ions onto the surfaces of the adsorbents, and it also minimises the energy barriers of reactions between the adsorbents and the adsorbates, which enhances the removal of phosphate (Liu *et al.* 2011). Additionally, some researchers claimed that increasing the ST could increase the solubility of iron and calcium oxides (from the adsorbents), which enhances the phosphate precipitation (Mezenner & Bensmaili 2009). Higher temperatures increase the relative motion of ions, which helps ions to escape from the adsorption sites (Xu *et al.* 2009).

The last examined parameter, in this study, was the dose of adsorbent (DoS). The results obtained from the commenced experiments proved that the DoS substantially affects the removal of phosphate by BA particles. For instance, the removal of phosphate was increased from the vicinity of 56% to the vicinity of 82% as the DoS increased from 35 to 55 mg/L, respectively, when the ST, HAC, and PoS were kept constant at 25 °C, 20 mg/L and 5, respectively. With increasing DoA, a larger number of active adsorption sites are available for phosphate adsorption, which enhances the removal efficiency (Xu *et al.* 2009).

In terms of the removal mechanism of phosphate from water using the BA particles, there are three main mechanisms. Firstly, the high content of SiO_2 (about 20% of the chemical composition) indicates that the physical adsorption of phosphate due to the presence of silicon results in a microporous structure of the material, which in turn increases the physical adsorption of phosphate (Zhou *et al.* 2019). Secondly, the presence of aluminium and iron oxides in the structure of BA promotes the chemosorption of phosphate at the active sites on the surface of BA particles (Yan *et al.* 2010). It should be mentioned that the SiO_2 plays an important role in the chemosorption of phosphate as it increases the surface area of the adsorbent, which in turn enhances subjected area for the chemical reactions between

phosphate and aluminium and iron oxides. Chemical precipitation of phosphate is the third predominant separation path due to the presence of calcium in the BA, which acts to precipitate phosphate (Zhou *et al.* 2019).

In summary, according to the results obtained from this study, the lowest adsorption of phosphate, 17.1%, was noticed at the lowest DoA (25 mg/L) and ST, HAC, and PoS of 30 °C, 30 mg/L, and 7, respectively. While the best adsorption of phosphate (83.8%) was noticed at the highest DoA (55 mg/L) and ST, HAC, and PoS of 35 °C, 20 mg/L, and 5, respectively.

A regression analysis was performed to assess the significance of each of the studied parameters in the adsorption of phosphate on the BA particles. The relative significances of the studied parameters, according to the outcomes of regression analysis, follow the order: DoA > PoS > HAC > ST, which means the DoA plays the most significant role in the adsorption of phosphate on the BA particles, followed by the PoS and HAC and ST.

Adsorption isotherm

As was mentioned above, assessment of the relationship between the adsorbed and aqueous concentrations is a basic step in the adsorption studies. Thus, the Langmuir model has been performed, in the present study, to assess the relationship between the adsorbed and aqueous concentrations of phosphate. Additionally, the separation factor has been calculated to evaluate the affinity between the phosphate and BA particles. Langmuir isotherm constants Q_o and b have been calculated by plotting C_e/q_e against C_e, as depicted in Figure 2. The obtained values of Q_o and b were 6.522 (mg/g) and 0.14 (L/mg), respectively.

According to Equation (8) and the calculated Langmuir isotherm constant, the R_L value for the adsorption of phosphate on the BA particles was 0.417, which confirmed that the adsorption of phosphate on BA particles was a favourable adsorption (Dada *et al.* 2012).

A glance at the outcomes of the present study could reveal that the present method has an edge over many of commonly used methods for phosphate removal because it does not require a long treatment time, it does not produce significant volumes of sludge, it helps to recycle waste in an eco-friendly way, and it does not deplete the natural resources. For instance, the literature shows that biological reactors are one of the commonly used methods for phosphate removal, and they enjoy good removal efficiency that could reach as high as 99% (Li *et al.* 2016). However, the biological methods require long treatment time, produce high volumes of sludge with high moisture content that requires expensive management strategies, which negatively influence its cost-effectiveness. In addition, biological reactors require precise and continuous monitoring to avoid the death of the bacteria (Camcıoğlu *et al.* 2019). In terms of advanced phosphate treatment methods, recent studies employed nanomaterials, such as nano-alumina, to achieve rapid and efficient phosphate removal from solutions. Although the nanomaterials demonstrated efficient removal of phosphate from solutions, the high cost of the nanomaterials and the possibility of releasing nanoparticles into the water being treated (toxicity) are the main limitations for this type of treatment method (Tyagi *et al.* 2018).

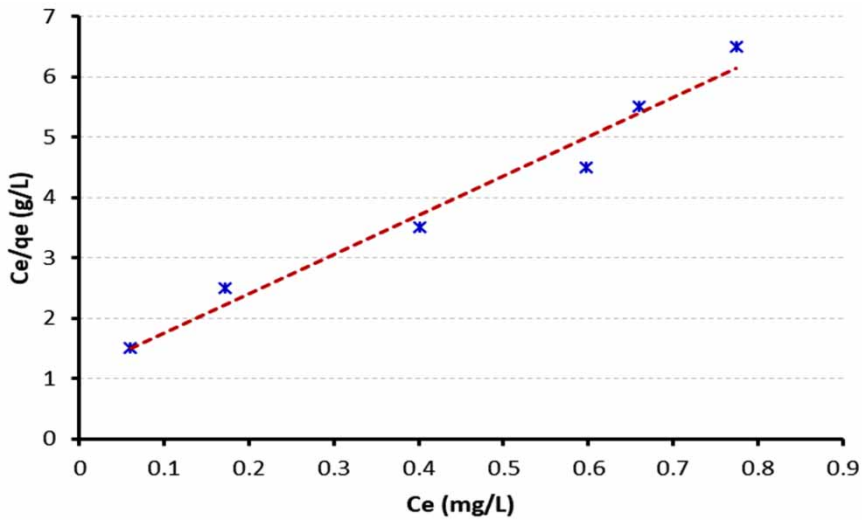

Figure 2 | Langmuir isotherm for phosphate adsorption on BA particles.

Modelling of phosphate adsorption on BA particles

The observed removals of phosphate on BA particles (Table 5) have been fed to CCD to yield a simulation equation that could be used, in future studies, to reproduce the removal of phosphate on BA particles without the need for commencing laboratory-based experiments. Thus, such simulation equations save both time and the cost of tests. The obtained simulation equation is shown in Equation (9).

$$\begin{aligned}\mathrm{Re}\% = {} & -40.79 + 1.31 \times \mathrm{ST} - 0.887 \times \mathrm{HAC} + 0.246 \\ & \times \mathrm{PoS} + 3.724 \times \mathrm{DoA} - 0.02308 \times \mathrm{ST}^2 + 0.0176 \times \mathrm{HAC}^2 \\ & - 0.5849 \times \mathrm{PoS}^2 - 0.03165 \times \mathrm{DoA}^2 + 0.001 \times \mathrm{ST} \times \mathrm{HAC} \\ & + 0.0037 \times \mathrm{ST} \times \mathrm{PoS} + 0.0025 \times \mathrm{ST} \times \mathrm{DoA} - 0.06062 \\ & \times \mathrm{HAC} \times \mathrm{PoS} - 0.0085 \times \mathrm{HAC} \times \mathrm{DoA} + 0.11313 \\ & \times \mathrm{PoS} \times \mathrm{DoA} \end{aligned} \quad (9)$$

It is noteworthy to highlight that the negative signs before the parameters or the combinations of parameters in Equation (9) are to highlight the negative impact of these parameters or combinations of parameters on the adsorption of phosphate on the BA particles, while the positive signs indicate positive impacts.

In fact, it is not necessary that every single parameter in Equation (9) makes a statistically significant contribution to the suggested model, where some of the parameters can be omitted from the suggested model due to their ignorable contribution (Pallant 2005; Hashim *et al.* 2017). The contribution of each parameter to the suggested model was assessed by determining its statistical significance (*p*-value). This parameter indicates whether this parameter makes a statistically significant contribution to the model or not; any parameter with a *p*-value less than 0.05 makes a significant unique contribution to the multiple regression model, while any parameter with a *p*-value more than 0.05 can be omitted from the model as it does not play a significant role (Pallant 2005; Hashim *et al.* 2017). According to the results of Table 6, three parameters, namely (ST × HAC), (ST × PoS), and (ST × DoA), can be omitted from the

Table 6 | Analysis of variance

Source	Degrees of freedom	Sequential sum of squares	Contribution	Adjusted sum of squares	Adjusted mean squares	P-value
Model	14	8,870.63	99.94%	8,870.63	633.617	0.000
Linear	4	8,196.06	92.34%	260.56	65.140	0.000
ST	1	5.23	0.06%	5.59	5.589	0.001
HAC	1	885.73	9.98%	14.09	14.091	0.000
PoS	1	1,994.73	22.47%	0.04	0.041	0.007
DoA	1	5,310.38	59.83%	214.90	214.902	0.000
Square	4	557.27	6.28%	557.27	139.318	0.000
ST*ST	1	1.82	0.02%	9.52	9.523	0.000
HAC*HAC	1	153.05	1.72%	88.62	88.620	0.000
PoS*PoS	1	116.03	1.31%	156.52	156.523	0.000
DoA*DoA	1	286.37	3.23%	286.37	286.375	0.000
2-Way interaction	6	117.30	1.32%	117.30	19.550	0.000
ST*HAC	1	0.04	0.00%	0.04	0.040	0.727
ST*PoS	1	0.02	0.00%	0.02	0.023	0.794
ST*DoA	1	0.25	0.00%	0.25	0.250	0.388
HAC*PoS	1	23.52	0.27%	23.52	23.522	0.000
HAC*DoA	1	11.56	0.13%	11.56	11.560	0.000
PoS*DoA	1	81.90	0.92%	81.90	81.903	0.000
Error	16	5.08	0.06%	5.08	0.318	–
Lack-of-fit	10	4.92	0.06%	4.92	0.492	0.001
Pure error	6	0.16	0.00%	0.16	0.027	–
Total	30	8,875.72	100.00%	–	–	–

model because their *p*-values are more than 0.05. Thus, the new formula of the suggested model is:

$$\begin{aligned}\text{Re}\% = &-40.79 + 1.31 \times \text{ST} - 0.887 \times \text{HAC} + 0.246 \times \text{PoS} \\ &+ 3.724 \times \text{DoA} - 0.02308 \times \text{ST}^2 + 0.0176 \times \text{HAC}^2 \\ &- 0.5849 \times \text{PoS}^2 - 0.03165 \times \text{DoA}^2 - 0.06062 \times \text{HAC} \\ &\times \text{PoS} - 0.0085 \times \text{HAC} \times \text{DoA} + 0.11313 \times \text{PoS} \times \text{DoA}\end{aligned} \quad (10)$$

The normal probability plot and versus order plots of the suggested model are shown in Figure 3.

To validate the developed model, it has been used to predict the adsorption of phosphate on the BA particles under the stated conditions in Table 5. The predicted removals of phosphate have been compared with the observed removals, see Table 7. Additionally, the coefficient of determination (R^2), which is an effective tool to assess the relationship between the predicted and observed phosphate removals,

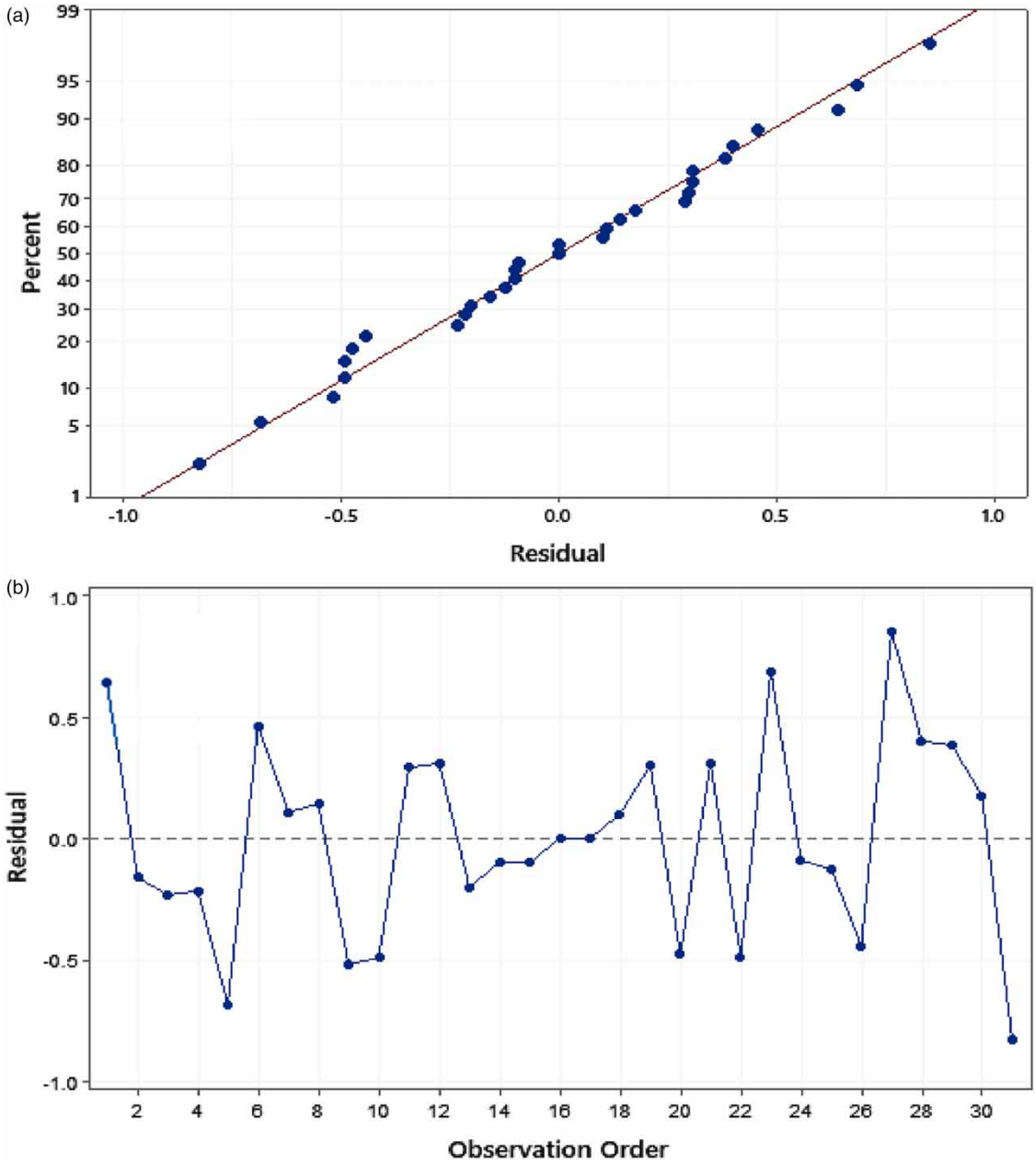

Figure 3 | (a) The normal probability plot, (b) versus order plot.

Table 7 | Predicted and observed phosphate removals by BA particles

Runs	Observed removal (%)	Predicted removal (%)	Runs	Observed removal (%)	Predicted removal (%)
1	57.4	53.38	17	60	59.99
2	22.4	22.54	18	60.1	59.99
3	35.3	35.53	19	60.3	59.99
4	47.6	47.81	20	68.4	68.88
5	54.2	54.86	21	77.4	77.08
6	56.4	55.94	22	78.7	79.19
7	71.2	71.08	23	24.1	23.40
8	71.4	71.24	24	36.1	36.19
9	82.1	82.61	25	48.4	48.52
10	17.1	17.59	26	55.8	56.22
11	32.7	32.39	27	57.3	56.45
12	55.2	54.88	28	72.7	72.29
13	59.8	59.99	29	72.8	72.40
14	59.9	59.99	30	83.8	83.62
15	59.9	59.99	31	57.8	58.62
16	60	59.99			

has been calculated by plotting the predicted phosphate removals against the observed removals, see Figure 4.

It can be seen from Table 7 that the observed removals of phosphate are in good agreement with the predicted removals. Additionally, the calculated value of R^2 was 0.99, which means the simulation model can reliably predict 99% of the effects of the studied parameters on phosphate removal by the BA particles.

CONCLUSIONS

The current study was devoted to investigating the applicability of industrial by-products, BA from power plants, to remove phosphate from water in the presence of competitor ions. The investigation was initiated by studying the chemical and physical characteristics of the BA to ensure that it has the potential ability to remove phosphate; that is, to check the content of iron and aluminium oxides and its surface area and density. Then, its ability to remove phosphate was validated by commencing sets of batch experiments under different conditions, including the DoA, PoS, ST and HAC. The kinetics of the adsorption process was also investigated using the Langmuir isotherm model. The outcomes of this study indicated that the BA sample contains considerable concentrations of iron, aluminium, and manganese oxides, which have good ability to remove phosphate from solutions, and it was found that the best performance of the BA particles could be attained in acidic solution, high dose of BA and in normal to moderate temperature levels (up to 35 °C). It was also found that both high pH and/or water temperatures negatively influenced the efficiency of the BA. Additionally, it was found that the presence of humic acid substantially minimised the adsorption of phosphate due to the competition for the adsorption sites. The adsorption isotherm study evidenced a high affinity between the BA particles and phosphate. Finally, it was found that the CCD could be efficiently used to model phosphate adsorption on BA.

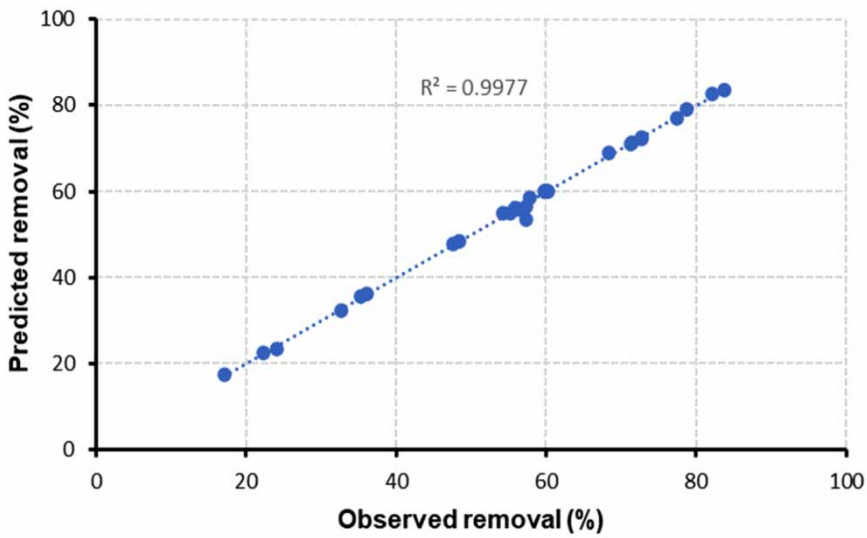

Figure 4 | Linear fit of the predicted and observed phosphate removals.

Generally, the outcomes of the present study could be preliminary evidence about the suitability of the BA particles, as economically efficient and eco-friendly adsorbent, for phosphate removal from water. For future studies, BA could be used to remediate water from other common pollutants, such as heavy metals and nitrates. Additionally, more studies should be commenced to develop adsorption mediums from industrial or agricultural by-products.

ACKNOWLEDGEMENTS

The authors are grateful to the research team from Al-Furat Al-Awsat Technical University and University of Babylon for carrying out the majority of the experiments during the lockdown period in the UK.

DATA AVAILABILITY STATEMENT

Data cannot be made publicly available; readers should contact the corresponding author for details.

REFERENCES

Al-Othman, Z. A., Ali, R. & Naushad, M. 2012 Hexavalent chromium removal from aqueous medium by activated carbon prepared from peanut shell: adsorption kinetics, equilibrium and thermodynamic studies. *Chemical Engineering Journal* **184**, 238–247.

Alwash, R. S. M. 2017 *Treatment of Highly Polluted Water with Phosphate Using BAPPP-Nanoparticles*. MSc thesis, Environmental Engineering, University of Technology, Iraq, Baghdad, Iraq.

Amini, M., Antelo, J., Fiol, S. & Rahnemaie, R. 2020 Modeling the effects of humic acid and anoxic condition on phosphate adsorption onto goethite. *Chemosphere* **253**, 1–10.

Boonamnuayvitaya, V., Sae-ung, S. & Tanthapanichakoon, W. 2005 Preparation of activated carbons from coffee residue for the adsorption of formaldehyde. *Separation and Purification Technology* **42** (2), 159–168.

Borggaard, O. K., Raben-Lange, B., Gimsing, A. L. & Strobel, B. W. 2005 Influence of humic substances on phosphate adsorption by aluminium and iron oxides. *Geoderma* **127** (3–4), 270–279.

Camcıoğlu, Ş., Özyurt, B., Şengül, S. & Hapoğlu, H. 2019 Evaluation of electro-Fenton method on cheese whey treatment: optimization through response surface methodology. *Desalination and Water Treatment* **172**, 270–280.

Dada, A., Olalekan, A., Olatunya, A. & Dada, O. 2012 Langmuir, Freundlich, Temkin and Dubinin–Radushkevich isotherms studies of equilibrium sorption of Zn^{2+} unto phosphoric acid modified rice husk. *IOSR Journal of Applied Chemistry* **3** (1), 38–45.

Dai, L. & Pan, G. 2014 The effects of red soil in removing phosphorus from water column and reducing phosphorus release from sediment in Lake Taihu. *Water Science and Technology* **69** (5), 1052–1058.

Gregg, S. & Sing, K. 1982 *Adsorption, Surface Area and Porosity*, 2nd ed. Academic Press, London.

Han, L., Xiao, T., Tan, Y. Z., Fane, A. G. & Chew, J. W. 2017 Contaminant rejection in the presence of humic acid by membrane distillation for surface water treatment. *Journal of Membrane Science* **541**, 291–299.

Hashim, K. S., Shaw, A., Al Khaddar, R., Ortoneda Pedrola, M. & Phipps, D. 2017 Defluoridation of drinking water using a new flow column-electrocoagulation reactor (FCER) - experimental, statistical, and economic approach. *Journal of Environmental Management* **197**, 80–88.

Hjelmar, O., Johnson, A. & Comans, R. 2010 Incineration: Solid Residues. In: *Solid Waste Technology and Management, Volume 1 and 2* (T. H. Christensen, ed.). John Wiley & Sons, Ltd, Chichester, UK.

Holden, J., Haygarth, P. M., MacDonald, J., Jenkins, A., Sapiets, A., Orr, H. G., Dunn, N., Harris, B., Pearson, P. L. & McGonigle, D. 2015 *Farming and Water 1: Agriculture's Impacts on Water Quality*. Global Food Security and UK Water Partnership, UK.

Jamaludin, S. S., Rani, N. A. & Mohamad, N. 2019 Investigation of water absorption and strength performances on concrete bricks containing Malaysian thermal power plant coal bottom ash (CBA). *Journal of Physics: Conference Series, IOP Publishing* **1349**, 1–6.

King, K. W., Williams, M. R. & Fausey, N. R. 2015 Contributions of systematic tile drainage to watershed-scale phosphorus transport. *Journal of Environmental Quality* **44** (2), 486–494.

Kirk, D. W., Jia, C. Q., Yan, J. & Torrenueva, A. L. 2003 Wastewater remediation using coal ash. *Integrated Management of Hazardous Waste* **5**, 5–8.

Kumar, P. S., Korving, L., van Loosdrecht, M. C. & Witkamp, G.-J. 2019 Adsorption as a technology to achieve ultra-low concentrations of phosphate: research gaps and economic analysis. *Water Research X* **4**, 100029.

Li, D., Lv, Y., Zeng, H. & Zhang, J. 2016 Enhanced biological phosphorus removal using granules in continuous-flow reactor. *Chemical Engineering Journal* **298**, 107–116.

Liu, J., Wan, L., Zhang, L. & Zhou, Q. 2011 Effect of pH, ionic strength, and temperature on the phosphate adsorption onto lanthanum-doped activated carbon fiber. *Journal of Colloid and Interface Science* **364** (2), 490–496.

Mezenner, N. Y. & Bensmaili, A. 2009 Kinetics and thermodynamic study of phosphate adsorption on iron hydroxide-eggshell waste. *Chemical Engineering Journal* **147** (2–3), 87–96.

Omran, I. I., Al-Saati, N. H., Hashim, K. S., Al-Saati, Z. N., Patryk, K., Khaddar, R. A., Al-Jumeily, D., Shaw, A., Ruddock, F. & Aljefery, M. 2019 Assessment of heavy metal pollution in the

Great Al-Mussaib irrigation channel. *Desalination and Water Treatment* **168**, 165–174.

Pallant, J. 2005 *SPSS Survival Manual*. Allen & Unwin, Australia.

Park, H., Nguyen, D. C. & Na, C.-K. 2015 Phosphate removal from aqueous solutions using (vinylbenzyl) trimethylammonium chloride grafted onto polyester fibers. *Water Science and Technology* **71** (12), 1875–1883.

Sellner, B. 2016 *Evaluating Steel Byproducts and Natural Minerals for Phosphate Adsorption From Agricultural Subsurface Drainage*. *MSc*, Civil Engineering, South Dakota State University, Brookings, SD, USA.

Shubbar, A. A., Jafer, H., Dulaimi, A., Hashim, K., Atherton, W. & Sadique, M. 2018 The development of a low carbon binder produced from the ternary blending of cement, ground granulated blast furnace slag and high calcium fly ash: an experimental and statistical approach. *Construction and Building Materials* **187**, 1051–1060.

Tyagi, S., Rawtani, D., Khatri, N. & Tharmavaram, M. 2018 Strategies for nitrate removal from aqueous environment using nanotechnology: a review. *Journal of Water Process Engineering* **21**, 84–95.

Viswanadham, B. V. S. 2016 *Soil Mechanics*. http://textofvideo.nptel.iitm.ac.in/105101084/lec7.pdf (accessed 08/02/2016).

Weng, L., Van Riemsdijk, W. H. & Hiemstra, T. 2012 Factors controlling phosphate interaction with iron oxides. *Journal of Environmental Quality* **41** (3), 628–635.

Withers, P. J., Neal, C., Jarvie, H. P. & Doody, D. G. 2014 Agriculture and eutrophication: where do we go from here? *Sustainability* **6** (9), 5853–5875.

Xu, X., Gao, B., Wang, W., Yue, Q., Wang, Y. & Ni, S. 2009 Adsorption of phosphate from aqueous solutions onto modified wheat residue: characteristics, kinetic and column studies. *Colloids and Surfaces B: Biointerfaces* **70** (1), 46–52.

Yan, L.-g., Xu, Y.-y., Yu, H.-q., Xin, X.-d., Wei, Q. & Du, B. 2010 Adsorption of phosphate from aqueous solution by hydroxy-aluminum, hydroxy-iron and hydroxy-iron–aluminum pillared bentonites. *Journal of Hazardous Materials* **179** (1–3), 244–250.

Zalidis, G., Stamatiadis, S., Takavakoglou, V., Eskridge, K. & Misopolinos, N. 2002 Impacts of agricultural practices on soil and water quality in the Mediterranean region and proposed assessment methodology. *Agriculture, Ecosystems & Environment* **88** (2), 137–146.

Zhang, B. & Poon, C. S. 2015 Use of furnace bottom ash for producing lightweight aggregate concrete with thermal insulation properties. *Journal of Cleaner Production* **99**, 94–100.

Zhao, B., Zhang, Y., Dou, X., Yuan, H. & Yang, M. 2015 Granular ferric hydroxide adsorbent for phosphate removal: demonstration preparation and field study. *Water Science and Technology* **72** (12), 2179–2186.

Zhou, H., Bhattarai, R., Li, Y., Li, S. & Fan, Y. 2019 Utilization of coal fly and bottom ash pellet for phosphorus adsorption: sustainable management and evaluation. *Resources, Conservation and Recycling* **149**, 372–380.

First received 1 July 2020; accepted in revised form 12 November 2020. Available online 27 November 2020